Journal of Computers Vol. 35 No. 5, October 2024, pp. 149-167
doi: 10.53106/199115992024103505011

An Average Temperature Feedback based PID Controller for Multi-Channel Balanced Heating in Thermal Vacuum Test

Xin Chang[1*], Bo Zang[1], Peng Gao[1], Xiaoke Li[1],
Zongmin Zhao[2], and Ao Ye[2]

[1] Environmental Testing Division, Beijing Institute of Space Mechanics and Electricity, Beijing, China

changxin198599@163.com, zangbo65536@126.com, gaopeng23231@163.com, lixiaoke1984535@163.com

[2] School of Information Communication Engineering, Beijing Information Science and Technology University, Beijing, China

vivzzm@163.com, 2022020566@bistu.edu.cn

Received 26 September 2024; Revised 2 October 2024; Accepted 19 October 2024

Abstract. With the development of aerospace technology, many devices under test (DUTs) in thermal vacuum tests require balanced heating. However, traditional PID controllers mostly focus on single-channel independent control, lacking effective solutions for the mutual influence among multiple channels. This paper proposes a PID controller based on average temperature feedback to address the issue of temperature imbalance in multi-channel heating. Firstly, this method calculates the difference between each channel's temperature and the average of all channels' temperature, and then feeds the difference into the input of the PID controller to real-time adjust the heating rates for each channel, ensuring balanced overall heating. Secondly, by detecting whether each channel has reached the lower limit of the set temperature range, the opportunity to exit the average temperature feedback is provided. Finally, a temperature acquisition and control synchronization system based on the EtherCAT network was built, providing an experimental platform for validating the proposed method. Through simulation and experimental validation, the proposed method not only reduces temperature difference among channels during the heating process, but also enhances the overall stability and robustness of the system. This makes it an effective solution for achieving precise thermal control in complex multi-channel environments.

Keywords: thermal vacuum test, multi-channel temperature control, PID controller

1 Introduction

In the development of modern aerospace and electronic equipment, thermal vacuum test (TVT) is a critical step to ensure that devices can operate normally under extreme environmental conditions [1, 2]. This is particularly important in the design and manufacturing of satellites, space probes, and high-altitude equipment, which often must withstand extreme temperature variations and near-vacuum environments [3]. Such conditions necessitate rigorous testing of the thermal management capabilities of these devices [4]. Thermal vacuum test simulates the vacuum and extreme temperature variations that equipment will encounter in space, effectively evaluating the thermal performance and structural reliability of the devices [5].

Typically, during a thermal vacuum test, a near-vacuum environment is provided for the device under test (DUT) to simulate the space environment. On this basis, the corresponding heaters are controlled to provide the DUT with high and low temperature environments for cyclical testing. The high-temperature test environment simulates the state when the DUT is exposed to sunlight in space, while the low-temperature test environment simulates the state when the DUT is not exposed to sunlight in space [6].

In thermal vacuum test, the appropriate heating method for DUT needs to be selected according to its type. For spacecraft and solar panels that are exposed to the space environment, infrared lamps are typically used for heating [7]. On the other hand, payloads that are installed inside the spacecraft generally require heating through thermal conduction methods. In thermal vacuum test that primarily rely on thermal conduction, many heating elements are attached to the DUT to provide uniform heating [8]. It is essential to maintain the entire device

* Corresponding Author

within the designed temperature range throughout the test to ensure the accuracy of the results and the safety of the equipment. When conducting thermal vacuum tests on spacecraft and their payloads, the temperature control system needs to regulate according to the DUT's extreme temperatures to verify if it can operate normally under these conditions [9]. Additionally, the system must strictly control overshoot and temperature imbalances between channels. Significant overshoot can cause the DUT to operate outside the permissible temperature range, potentially damaging it. Excessive temperature differences between channels can lead to thermal stress on the DUT, causing local deformation and, in severe cases, irreversible damage.

In the field of industrial control, the Proportional-Integral-Derivative (PID) controller is one of the most technically mature and widely used control regulators. The PID controller adjusts the system output to bring it closer to the setpoint, correcting system errors through three basic functions: proportional, integral, and derivative. Proportional control adjusts based on the current error value, that the larger the error, the greater the adjustment effort, which aids in quickly responding to changes [10]. However, using it alone may not eliminate steady-state error. Integral control adjusts based on the accumulation of errors over time, aiming to eliminate steady-state error. Integral control can induce overshoot and oscillations of the system. Hence, it requires careful tuning. Derivative control adjusts based on the rate of change of the error, serving to reduce error change trends, thus enhancing the system's dynamic response and helping to reduce overshoot.

When using a PID controller for system regulation, parameter tuning is a crucial step to ensure system stability and optimize performance. The three parameters of a PID controller, which are proportional gain, integral time, and derivative time, determine the system's response characteristics. Proper parameter configuration can ensure that the system responds quickly, remains stable, and minimizes oscillation or overshoot [11]. However, in each thermal vacuum test, the DUTs are not same, the number and layout of heaters as well as temperature sensors are different. This necessitates tuning the three PID controller parameters for each test. Undoubtedly, this parameter tuning can consume a significant amount of test time, which is intolerable for organizations that need to conduct numerous tests annually. Therefore, some adaptive PID algorithms have been applied in the field of thermal vacuum test. These algorithms can adjust the PID parameters in real-time during the control process, enabling the control system to operate stably.

However, simultaneously controlling the temperature of multiple channels remains a significant challenge for temperature control systems. A multi-channel temperature control system must not only monitor and precisely adjust multiple temperature points in real-time but also manage the thermal coupling effects between different channels, which adds complexity to the system's design and optimization [12]. While traditional single-input single-output (SISO) control methods offer some resistance to external disturbances [13], the thermal interactions between channels can exacerbate interference, potentially leading to temperature oscillations that prevent the system from stabilizing within the desired temperature range [14].

Therefore, investigating how to achieve high-precision multi-channel temperature control under thermal vacuum testing conditions has become a crucial topic for improving test accuracy and equipment reliability. In thermal vacuum test, multi-channel temperature control tends to cause temperature differences between channels during the heating process. This paper proposes a multi-channel PID controller based on average temperature feedback to address the issue of temperature imbalance between channels during the heating process in thermal vacuum tests. The main contributions of this paper are as follows:

(1) Optimize the PID controller by using the average value of the current temperatures across multiple channels as one of the feedback inputs for each channel's PID controller, to adjust the differences between that channel and the others in real-time.

(2) Providing a mechanism for exiting average temperature feedback in multi-channel temperature control, allowing for a smooth transition to traditional PID control after the heating phase.

(3) A temperature control system based on EtherCAT was set up, integrating all the temperature acquisition and control circuits into the EtherCAT network. This enables synchronized temperature acquisition and control, ensuring consistent time intervals for temperature control.

The remainder of this paper is organized as follows: Chapter 2 introduces related work. Chapter 3 presents the main content of the proposed method. Chapter 4 provides a simulation validation of the proposed method. Chapter 5 demonstrates the experimental results of applying the proposed method for multi-channel temperature control in an actual thermal vacuum environment. Chapter 6 concludes the paper.

2 Related Work

There has been considerable exploration and progress in the application of multi-channel temperature control technology in thermal vacuum test. Traditional temperature control techniques primarily rely on PID controllers, which adjust the proportional, integral, and derivative parameters to achieve stable temperature control across a wide range of applications [15, 16]. However, when it comes to multi-channel temperature control, particularly in thermal vacuum environments, the nonlinearity of system and thermal coupling effects between channels make it challenging for PID controllers to achieve optimal control performance [17]. To address this issue, researchers have proposed several improved methods, such as adaptive PID control and self-tuning PID control [18, 19]. Adaptive PID control introduces a parameter adaptation mechanism, allowing the PID controller to adjust its parameters in real-time according to changes in the system state [20]. Self-tuning PID control, on the other hand, is a self-optimization method based on real-time feedback. By monitoring the system's response characteristics, the self-tuning PID controller can automatically adjust the control parameters without manual tuning, thereby improving the flexibility and accuracy of the control system [21]. These methods introduce mechanisms for parameter adaptation or model-based correction strategies, which enhance the response speed and accuracy of the control system to a certain extent.

In recent years, with the advancement of computational capabilities and control algorithms, advanced control theories have increasingly been applied to multi-channel temperature control. Methods such as Model Predictive Control (MPC) [22, 23]and Fuzzy Logic Control (FLC) [24] have gained significant attention due to their ability to handle multivariable coupling and nonlinear systems. MPC achieves high precision and response speed in multi-channel temperature control by predicting future system states and optimizing current control inputs based on a predefined objective function. Reference [25] explores the integration of fuzzy logic with model predictive control for managing nonlinear processes. However, the computational complexity of MPC is relatively high, particularly in real-time control, requiring substantial computational resources and time, which limits its practical application in thermal vacuum testing. On the other hand, FLC addresses system uncertainties and nonlinear characteristics through fuzzy rules. FLC can address the thermal coupling effects between channels through fuzzy rules, and it exhibits good adaptability when dealing with system parameter changes during testing. YL Huang introduced a fuzzy model predictive control (FMPC) approach to design a control system for a highly nonlinear process [26]. While FLC can achieve effective control under certain conditions, the formulation of these rules depends on expert experience, making it difficult to widely generalize.

In addition, Neural Network Control (NNC) [27, 28] and Deep Learning Control (DLC) [29, 30], which have emerged as intelligent control methods in recent years, are also beginning to show potential in the field of multi-channel temperature control. NNC adapts control strategies by learning the input-output relationships of the system, demonstrating strong adaptability when dealing with complex multi-channel temperature control problems. In reference [31], actor-Critic learning was used to tune PID parameters in an adaptive way by taking advantage of the model-free and on-line learning properties of reinforcement learning effectively. DLC further leverages the representational power of deep neural networks, excelling in both control precision and adaptability to complex scenarios. Wang peng proposed a PID approach for accelerating deep network optimization. This approach first reveals the intrinsic connections between SGD-Momentum and PID based controller, then present the optimization algorithm which exploits the past, current, and change of gradients to update the network parameters [32]. However, these methods also face challenges such as high computational costs and the need for large amounts of training data, and their application in thermal vacuum testing is still in the exploratory stage.

In summary, although multi-channel temperature control technology has a certain research foundation in thermal vacuum testing [33, 34], existing methods still face challenges in response speed, control accuracy, and computational resource requirements. As aerospace technology advances, the demands on temperature control continue to increase, prompting researchers to explore more effective and efficient control strategies to meet the increasingly complex testing requirements. Therefore, this paper proposes a multi-channel temperature control algorithm based on an average temperature feedback strategy, aiming to achieve balanced temperature rise across channels during the heating process, thereby enabling the surface temperature of the device under test to uniformly reach the set temperature.

3 Proposed Method

This section mainly introduces the temperature control system under thermal vacuum test, the transfer function

of heating system based on heating plates and the proposed multi-channel temperature controller.

3.1 The Structure of Temperature Control System

The environment of thermal vacuum test consists of a vacuum tank, the DUT, the heating plates, and T-type thermocouples, shown as Fig. 1. Among them, the vacuum tank is the main equipment for conducting thermal vacuum test, which continuously extracts air through an external vacuum pump to make its interior close to a vacuum environment. The DUT with a large number of heating plates and T-type thermocouples installed on the surface will be placed in vacuum tank for corresponding tests. The heating plates and thermocouples are arranged according to the designer's requirements. In addition, during the thermal vacuum test, the liquid nitrogen is injected into the interlayer of the outer wall of the vacuum tank to provide heat sink. The heating plate is controlled by programmable power supply outside the vacuum tank, and the T-type thermocouple is also connected to the external temperature sampling circuit.

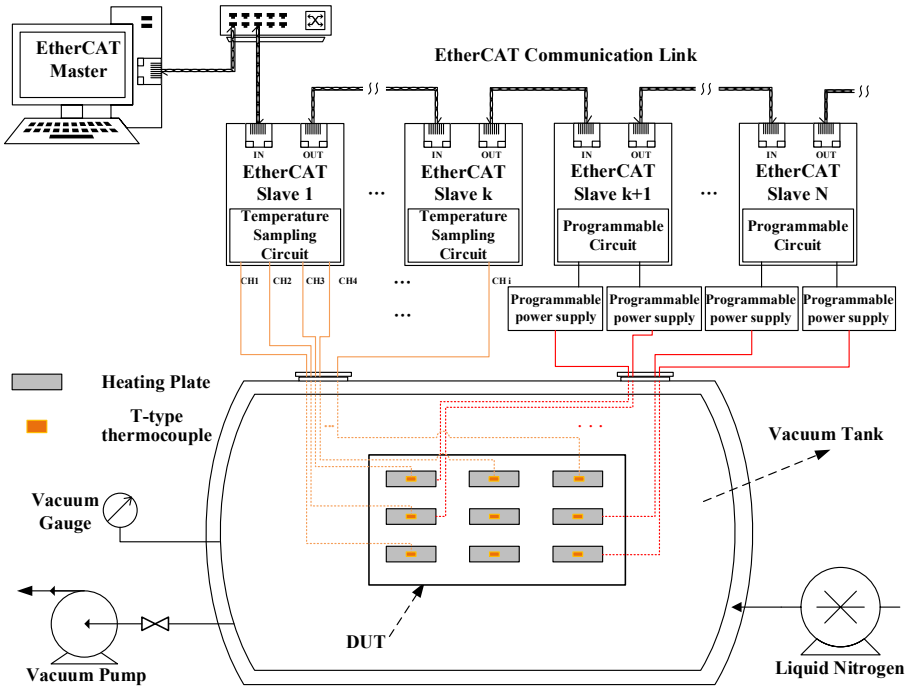

Fig. 1. The structure of thermal vacuum test

In order to access a large number of temperature acquisition devices and power devices, thermal vacuum test systems typically use conventional Ethernet methods to connect all devices via a switch, with the control program running on a server that is also connected to this network. During temperature control, the server inputs the temperature values of all valid channels into the corresponding PID control programs and calculates the current values required for each channel. These current values are sequentially sent to each programmable power supply through Ethernet to achieve temperature control. However, in the process of sending current values to each programmable power supply via Ethernet, the control program needs to wait for the response signal from the power device before sending the current value for the next channel. When the number of channels is large, the cumulative response time gradually increases, which affects the interval and consistency of temperature control, ultimately impacting the accuracy of temperature regulation.

In order to improve channel consistency and reduce control intervals for multi-channel controlling, this system is designed with a temperature acquisition and programmable power control circuit based on EtherCAT technology. EtherCAT is a high-performance real-time industrial Ethernet solution that enables high-speed communication and control of industrial automation devices through standard Ethernet technology. Unlike traditional Ethernet protocols, EtherCAT employs "processing on the fly" for data handling. This means that data frames are processed and immediately forwarded by the slave devices as they pass through, rather than being received in their entirety before processing. This approach significantly reduces communication latency and enhances data transmission efficiency. Each data frame processing takes only a few nanoseconds, allowing EtherCAT to support real-time updates of up to thousands of I/O points, with cycles under 100 microseconds.

The control system in this document is designed with dedicated temperature acquisition circuits and programmable power control circuits. Both of these circuits support the EtherCAT protocol and facilitate communication with the EtherCAT master station. The master station primarily handles network configuration and initiates data communication packets for every slave station. The slave station is connected to the master station through a switch in open connection mode, that these slave stations within the same switch network segment are treated as one Ethernet device for addressing. Different slave stations within the same network segment are addressed through sequential mode. Besides, the master station operates in periodic mode to ensure that all slave stations can synchronously perform temperature acquisition and temperature control operations.

3.2 The Transfer Function of Heating System

The model of the heating plate temperature control system in a thermal vacuum test can typically be approximated as a First-Order Plus Dead Time (FOPDT) model, with its transfer function given by the following equation:

$$G(s)=\frac{K}{Ts+1}e^{-\tau s} \quad . \tag{1}$$

Here, K denotes the magnification factor, T presents the time constant, and τ is time delay.

In industrial control applications, the step response method is typically used to solve for K, T, and τ in equation (1). The step response method is an important tool for analyzing the dynamic characteristics of linear time-invariant systems. By introducing a unit step function as the system input, the system produces a corresponding output response that varies over time. Eventually, its step response will reach a new steady-state value. By observing the output response curve, one can evaluate the system's dynamic performance and adjust control parameters to achieve the desired behavior.

In the experimental environment of Section 3.1, the step response method is utilized to determine the transfer function of temperature control system, that is, to fit the system's transfer function based on the temperature change curve under a fixed amplitude current output. In the Laplace domain, the system response $F(s)$ of the temperature control system is related to the system's transfer function $G(s)$ and the control signal $U(s)$, which can be expressed as:

$$F(s)=G(s)U(s) \tag{2}$$

$$U(s)=\frac{U_0}{s} \tag{3}$$

Where, U_0 denotes the amplitude of the step input. Substituting equations (1) and (3) into equation (2) gets the following equation:

$$F(s)=\frac{K}{Ts+1}e^{-\tau s}\cdot\frac{U_0}{s} \tag{4}$$

By applying the inverse Laplace transform to F(s), the transient response of the control system in the time domain can be obtained, which is shown as

$$f(t)=\mathcal{L}^{-1}\left[F(s)\right]=\begin{cases}K\cdot U_0\cdot\left(1-e^{\frac{\tau-t}{T}}\right), t\geq\tau\\ 0, \qquad\qquad t<\tau\end{cases}. \tag{5}$$

Here, $\mathcal{L}^{-1}$ denotes the inverse Laplace transformation. The value of K could be calculated by the following equation:

$$K=\frac{f(\infty)-f(0)}{u(\infty)-u(0)} \tag{6}$$

Where, $f(\infty)$ and $u(\infty)$ represent system response value and the input amplitude at the steady state, respectively. $f(0)$ and $u(0)$ denote system response value and the input amplitude at the initial state, separately.

Additionally, it is necessary to record the corresponding values of $f(t_1)$ and $f(t_2)$ at two known time points t_1 as well as t_2, and establish the following system of equations to solve for the values of t and τ.

$$\begin{cases}\dfrac{f(\infty)-f(t_1)}{f(\infty)}=e^{\left(\frac{\tau-t_1}{T}\right)}\\ \dfrac{f(\infty)-f(t_2)}{f(\infty)}=e^{\left(\frac{\tau-t_2}{T}\right)}\end{cases} \tag{7}$$

Based on the above formulas, a constant input current (2A) was provided to the heating plate-based temperature control system. By recording the corresponding temperature response, the values of the relevant parameters are determined: K = 72.83, T = 121.71, τ = 2.3. Therefore, the transfer function of the heating system is represented by the following equation:

$$G(s)=\frac{72.83}{121.71s+1}e^{-2.3s} \tag{8}$$

3.3 ATF-PID Controller

In thermal vacuum tests, traditional PID control regulates temperature based on the error between the current temperature value of each DUT channel and the set value, as shown in Fig. 2. In Fig. 2, $r(t)$ represents the final stabilized value of the controlled channel, which is usually preset before the system executes control. $y(t)$ is the current response of the channel, namely the temperature value at the test point collected by the current channel's temperature sensor. The deviation between the current response $y(t)$ and the set value $r(t)$ is represented by $e(t)$. The PID controller $C(s)$ computes the control output $u(t)$ through a combined operation of proportional, integral, and derivative actions on $e(t)$, as shown in equation (9).

$$u(t)=K_P\cdot e(t)+K_I\cdot\int_0^t e(v)dv+K_D\cdot\frac{de(t)}{dt} \tag{9}$$

Where K_P, K_I, and K_D are the proportional, integral, and derivative coefficients, respectively, which need to be tuned in advance. The control variable $u(t)$ is the current supplied to the heater at this time by the programmable power supply.

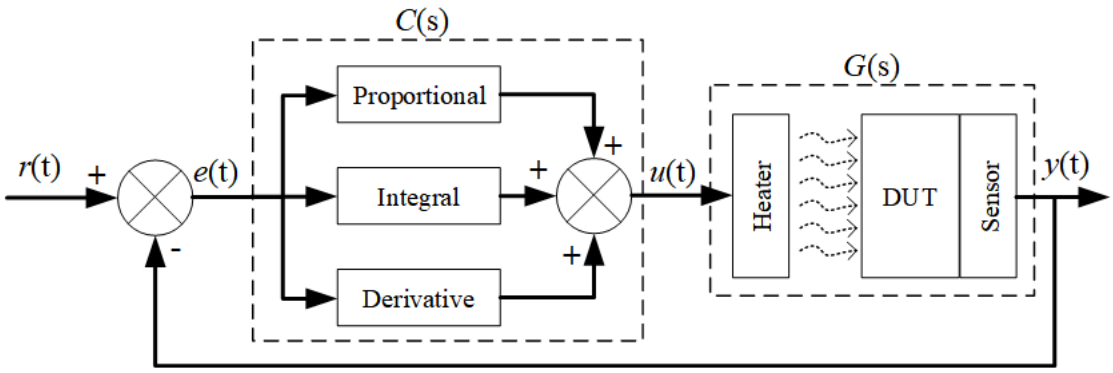

Fig. 2. Traditional PID architecture for temperature control

After the current $u(t)$ is input into the heater, the heater generates corresponding heat, which is conducted to the DUT, causing a change in the DUT's temperature. Finally, the temperature values at each control point on DUT are obtained through corresponding sensor as well as acquisition circuit. These values are fed back to the input of the control channel and compared with $r(t)$ to obtain $e(t)$, thereby forming a closed-loop control system.

In practical applications, equation (9) is not easy to implement due to the presence of integral and derivative operations. To facilitate computation, the PID controller in continuous time is often discretized for use in actual digital control systems. The discretized formula of PID controller at moment k is as follows:

$$u(k) = K_P \cdot e(k) + K_I \cdot \sum_{j=0}^{k} e(j) + K_D \cdot \left(e(k) - e(k-1)\right) . \tag{10}$$

Here, $u(k)$ represents the control output at the moment k, and k denotes the number of samplings. $e(k)$ and $e(k-1)$ indicate the deviation between the system response and the set temperature value at the current moment k and previous moment k-1, respectively. $\Sigma_{i=0}^{m} e(i)$ represents the accumulation of all errors $e(j)$ from the start of control to the current moment k.

In the traditional independent channel control strategy, each channel's PID controller only adjusts the temperature control response for the corresponding channel. In this case, the controller adjusts based on how quickly the corresponding channel reaches the set value, without considering the temperature differences among channels. Due to the uneven layout of the heating plates and certain performance differences among them, the response of each channel during the heating process would be different, leading to inconsistent temperatures across channels at the same moment. A very obvious example is that heating plates located in center area typically have a higher heating rate and thus higher temperatures compared to those positioned at the edges. If this is not controlled, it could lead to an increasing temperature difference between adjacent area on the DUT, potentially affecting the DUT's performance.

To address this issue, a PID controller based on average temperature feedback is proposed, with its basic architecture shown in Fig. 3. This controller is divided into two main parts: the general PID controller and the average feedback. The general PID controller is mainly used to implement temperature control for each channel. The controller's error $e(t)$ not only includes the deviation between the current response and the set value for each channel but also the deviation between the response of each channel and the average response of all channels. The average feedback part calculates the average response of all channels, providing each channel with the deviation from the average response. The average feedback part also offers the timing for the average feedback mechanism to exit. The specific implementation of these two parts is described as follows.

(1) The General PID Controller

The general PID controller part is mainly used for implementing temperature control. For multi-channel temperature control, each temperature measurement point that needs to be controlled requires a complete set of acquisition circuitry, heaters, and control programs to achieve closed-loop temperature control.

Assume that in a thermal vacuum test, there are N temperature control points on the DUT that need to be monitored, with each control point presetting a target temperature of $T_{set}(t)$. To control the temperature at these points, N sets of sensors, acquisition equipment and programmable power supplies are needed, with N sets of PID controllers loaded into the control program.

At moment k, for the i-th channel, the error input $e_i(k)$ of its PID controller can be expressed as the deviation between the current system temperature response $y_i(k)$ and the preset value $T_{set}(k)$, minus the average deviation $\overline{e}_i(k)$ of the i-th channel, as shown in the following formula.

$$e_i(k) = T_{set}(k) - y_i(k) - \overline{e}_i(k),\ i = 1,2,\ldots N \tag{11}$$

Here, $\overline{e}_i(k)$ represents the difference between the response $y_i(k)$ of the i-th channel and the average response $\overline{y}(k)$ of all channels, as shown in the following equation.

$$\overline{e}_i(k) = y_i(k) - \overline{y}(k) \tag{12}$$

According to equation (10), the discrete PID control formula for each channel can be derived as

$$u_i(k) = K_P \cdot e_i(k) + K_I \cdot \sum_{j=0}^{k} e_i(j) + K_D \cdot \left(e_i(k) - e_i(k-1)\right) . \tag{13}$$

Due to the accumulation component from the beginning to the present in the discrete PID control described in equation (13), the computational complexity is relatively high. To optimize computational efficiency, the control quantity can be decomposed by only calculating the change in control quantity, resulting in an incremental PID controller. Substituting $k = k$-1 into equation (13), we obtain the following formula:

$$u_i(k-1) = K_P \cdot e_i(k-1) + K_I \cdot \sum_{j=0}^{k-1} e_i(j) + K_D \cdot \left(e_i(k-1) - e_i(k-2)\right) . \tag{14}$$

Equation (13) minus equation (14), the following formula is obtained.

$$u_i(k) - u_i(k-1) = K_P \cdot \left(e_i(k) - e_i(k-1)\right) + K_I \cdot e_i(k) + K_D \cdot \left(e_i(k) - 2e_i(k-1) + e_i(k-2)\right) \tag{15}$$

By moving $u_i(k-1)$ to the right side of the equation, the incremental PID control formula for each channel is derived, which only relates to the errors from the most recent three samples.

$$u_i(k) = u_i(k-1) + K_P \cdot \left(e_i(k) - e_i(k-1)\right) + K_I \cdot e_i(k) + K_D \cdot \left(e_i(k) - 2e_i(k-1) + e_i(k-2)\right) \tag{16}$$

(2) The Average Temperature Feedback

The average temperature feedback part is primarily used to provide each channel with the deviation between its temperature and the temperatures of other channels. This ensures that the channels which are heating up too quickly slow down their heating rate, while the channels which are heating up too slowly try to increase their heating rate. This allows all channels to heat up evenly at any given moment.

In the thermal vacuum test, to ensure that all channels can heat at a more similar rate, we selected the average value of the output responses from all channels as the measurement standard. As can be seen from equation (11), the difference between the proposed method and the traditional independent control method lies in the fact that the input to the PID controller also subtracts the deviation between the current channel temperature and the average temperature, which is defined as the average deviation $\overline{e}_i(k)$. Therefore, the key to the proposed method is the introduction of the average deviation.

In the process of multi-channel temperature control, the average value of the output responses from all channels is utilized as the criterion for evaluating whether each channel is heating up too quickly or too slowly, which is denoted as $\overline{y}(k)$:

$$\overline{y}(k)=\frac{1}{N}\sum_{i=1}^{N}y_i(k) \ . \tag{17}$$

Here, N presents the number of all channels for the temperature control system, and $y_i(k)$ denotes the system response of the i-th channel. By comparing the current system response $y_i(k)$ of each channel with $\overline{y}(k)$, it is possible to determine whether the temperature of that channel was too high or not. The difference between $y_i(k)$ and $\overline{y}(k)$ is defined as the average temperature deviation:

$$e_i^{'}(k)=y_i(k)-\overline{y}(k) \ . \tag{18}$$

In multi-channel temperature control, significant temperature differences among channels often occur during the heating phase. Once the temperature values of each channel reach the set value one after another, the channels, which reach the set temperature earlier, will still have their average deviation $\overline{e}_i(k)$ subtracted from the input term of their PID controller. This will ultimately lead to all channels stabilizing at a temperature slightly deviating from the set value, preventing the thermal vacuum test from evaluating the DUT at the expected temperature. Considering that once all channels are uniformly heated to near the set temperature, the temperature differences among channels become very small, and the traditional PID algorithm can effectively control each channel to the preset temperature and maintain stability, it is crucial to exit the average temperature feedback strategy in the final stages of heating. The timing for exiting this strategy will be discussed below.

Typically, in thermal vacuum tests, a target temperature is set for each channel along with a tolerance range for that target temperature. The temperature tolerance is always provided alongside the preset temperature to protect the equipment. For instance, if the target temperature is set at 60°C, the actual control temperature can fluctuate within 2°C above or below 60°C, meaning the permissible temperature range is [58°C, 62°C]. In this paper, the timing for disengaging the average temperature feedback from the temperature control system is determined by the channel that first reaches the lower limit of the set temperature range. When the first channel reaches the lower limit of the temperature control range during the heating process, the average temperature feedback would be disconnected for all channels within the PID controller. At this point, for channels with temperatures higher than the average temperature $\overline{y}(k)$, the increased input error $e_i(k)$ to the PID controller will accelerate the heating rate, which would be quickly adjusted by the PID controller. For other channels, as $e_i(k)$ decreases, the control current will be further reduced, minimizing the risk of overshooting. Additionally, as the current in the latter channels decreases, it also reduces the influence on the temperatures of the former channels. To this end, a variable S is defined to determine whether the temperature control system needs to integrate the average temperature feedback, with the formula as follows:

$$S=\begin{cases}1, \ max\{y_1(k),y_2(k),\ldots,y_N(k)\}\geq T_{set}^{min}\\ 0, \ max\{y_1(k),y_2(k),\ldots,y_N(k)\}<T_{set}^{min}\end{cases} \ . \tag{19}$$

Where $T_{set}^{\min}$ represents the lower limit of the preset temperature range. Based on the value of S, $\overline{e}_i(k)$ can be expressed as:

$$\overline{e}_i(k)=\begin{cases}e_i^{'}(k), & S=0\\ 0, & S=1\end{cases} \ . \tag{20}$$

Therefore, the input $e_i(k)$ for the PID controller in each channel is expressed as:

$$e_i(k) = T_{set}(k) - y_i(k) - e_i'(k) \,\&\, \bar{S},\ i = 1,2,\ldots N \tag{21}$$

Based on equation (16), (19), and (21), iterative updates can be performed to achieve temperature balance control across multiple channels.

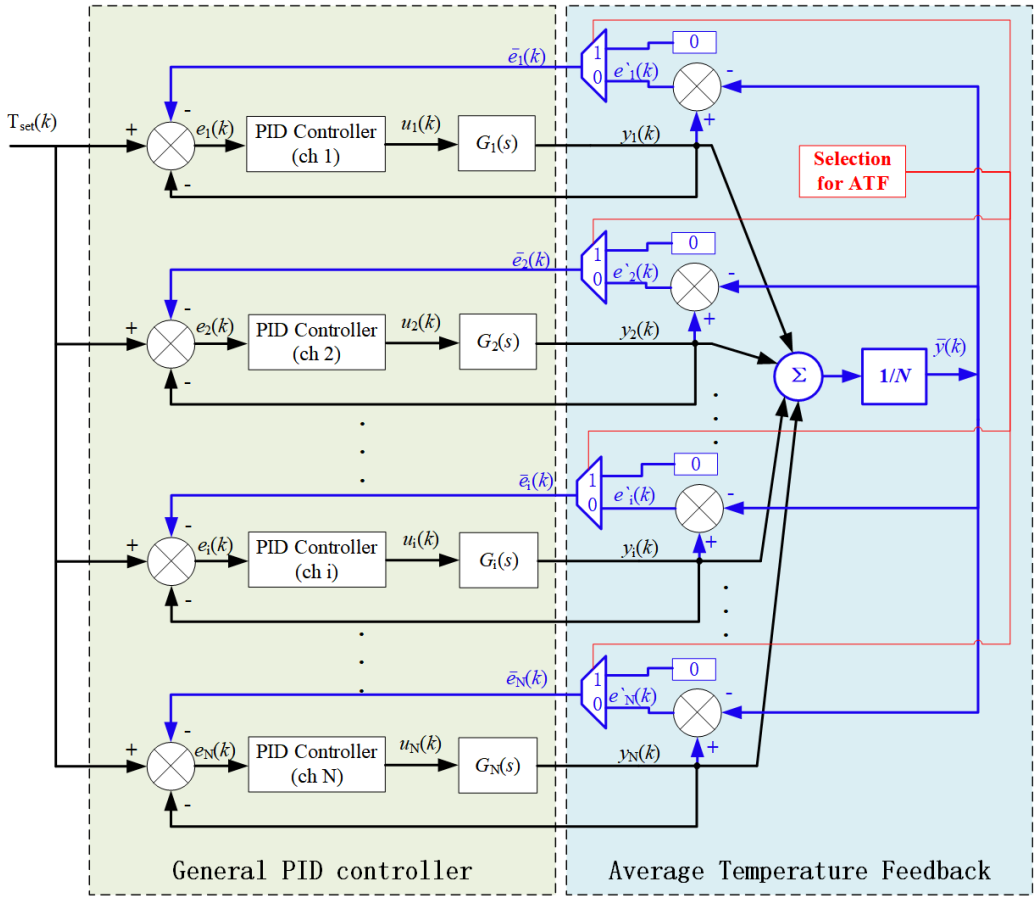

Fig. 3. The structure of average temperature feedback based PID controller

4 Simulation

In order to validate the proposed method, we designed a temperature control simulation for a 3×3 array and compared the temperature differences among channels when using the proposed method and when not using it.

4.1 Simulation Setup

To verify the proposed algorithm's effectiveness in suppressing inter-channel interference, we conducted a simulation by using nine temperature control channels, arranged in a 3×3 array. The layout of these channels and their numbering are shown in Fig. 4.

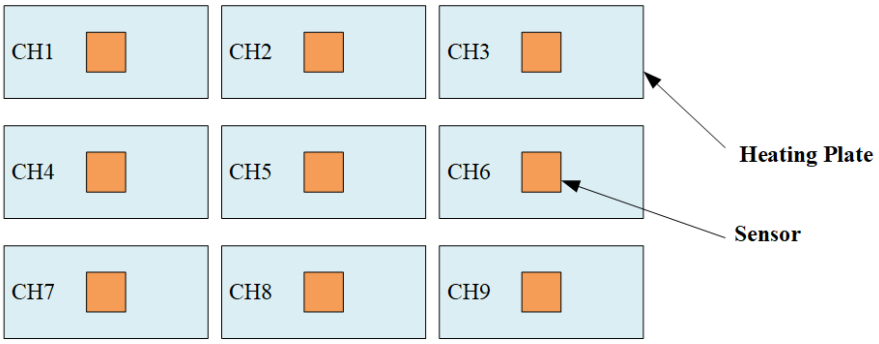

Fig. 4. The layout diagram of the heating plates and sensors for multi-channel temperature control system

Based on the above layout, we have provided the coupling coefficient representing the mutual temperature influence between channels:

$$\alpha = \begin{bmatrix} 0.3 & 0.05 & 0 & 0.05 & 0.02 & 0 & 0 & 0 & 0 \\ 0.05 & 0.3 & 0.05 & 0.02 & 0.05 & 0.02 & 0 & 0 & 0 \\ 0 & 0.05 & 0.3 & 0 & 0.02 & 0.05 & 0 & 0 & 0 \\ 0.05 & 0.02 & 0 & 0.3 & 0.05 & 0 & 0.05 & 0.02 & 0 \\ 0.02 & 0.05 & 0.02 & 0.05 & 0.3 & 0.05 & 0.02 & 0.05 & 0.02 \\ 0 & 0.02 & 0.05 & 0 & 0.05 & 0.3 & 0 & 0.02 & 0.05 \\ 0 & 0 & 0 & 0.05 & 0.02 & 0 & 0.3 & 0.05 & 0 \\ 0 & 0 & 0 & 0.02 & 0.05 & 0.02 & 0.05 & 0.3 & 0.05 \\ 0 & 0 & 0 & 0 & 0.02 & 0.05 & 0 & 0.05 & 0.3 \end{bmatrix} \tag{22}$$

In addition, considering that each channel is subject to certain environmental influences in practical situations, a noise with $\mathcal{N}(0, 1)$ has been provided for each channel.

We set the initial temperature of these nine channels to 20°C, with a target temperature of 90°C and a target temperature range of [87°C, 93°C]. The corresponding simulation verification is conducted under these conditions.

4.2 Simulation Result

In this simulation, the feasibility of the proposed method is verified by comparing with the traditional PID algorithm under the condition 1, whose PID control parameters for each channel are as follows:

$$\begin{cases} K_P = 0.0317 \\ K_I = 0.0003 \\ K_D = 0.0021 \end{cases}. \tag{23}$$

Fig. 5 illustrates the heating control effectiveness of the traditional PID algorithm under multi-channel conditions. As shown in the figure, there is a significant temperature difference among the channels during the heating process. The central channel, Channel 5, is most influenced by the other channels, leading to the highest temperature during the heating process and the largest temperature difference compared to the other channels. Fig. 6 shows the temperature difference between Channel 5 and the other channels under this condition. It is clear from the figure that the temperature difference between Channel 5 and the other channels ranges from [0°C, +11°C].

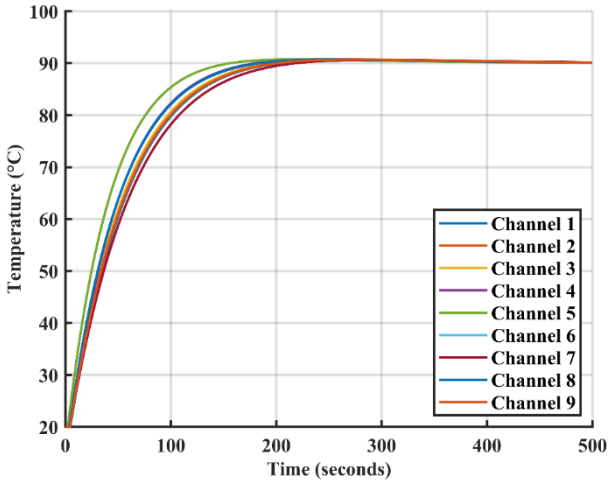

Fig. 5. The multi-channel control effects of PID algorithm under condition 1

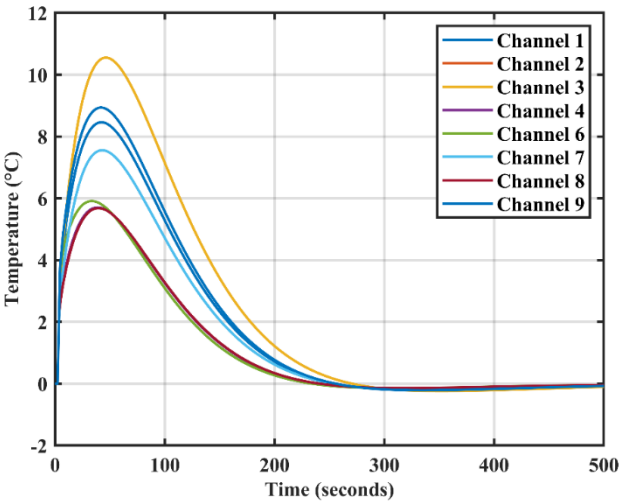

Fig. 6. The temperature difference of PID algorithm under multi-channel condition 1

Fig. 7 demonstrates the heating control performance of the proposed ATF-PID algorithm under multi-channel conditions. To ensure a fair comparison with the PID algorithm, the PID control parameters used in the proposed method are the same as those used in Fig. 5 and Fig. 6. As shown in Fig. 7, the temperature differences among the channels during the heating process are effectively suppressed. Although the temperature of Channel 5 remains the highest during the heating process, the temperature difference between it and the other channels has been significantly reduced. Fig. 8 shows the temperature difference between Channel 5 and the other channels under this condition, with the temperature difference range narrowed to within [0°C, +4.2°C].

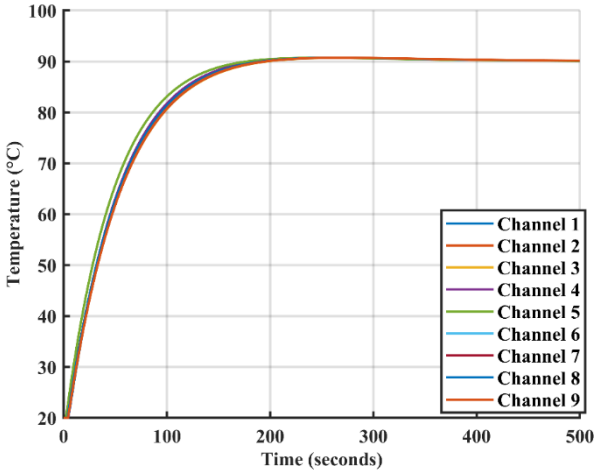

Fig. 7. The multi-channel control effects of ATF-PID algorithm under condition 1

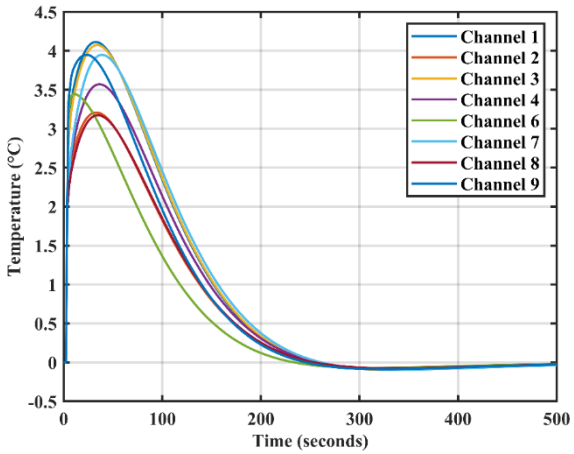

Fig. 8. The temperature difference of ATF-PID algorithm under multi-channel condition 1

To further verify the effectiveness of the proposed method in the temperature control process, a more aggressive control process is used for comparison. The new control process will result in a faster temperature rise, with a little overshoot. The relevant coefficients of the condition 2 are as follows:

$$\begin{cases} K_P = 0.07 \\ K_I = 0.00075 \\ K_D = 0.001 \end{cases}. \tag{24}$$

At first, Fig. 9 shows the control effect of the traditional PID under Condition 2. It can be seen that, compared to Condition 1, the overall heating speed of the system under Condition 2 is faster, but some overshoot has also occurred. Due to its central position, Channel 5 remains the fastest heating channel. The faster heating rate under Condition 2 also leads to greater temperature differences among the channels. As shown in Fig. 10, the maximum temperature difference between Channel 5 and the other channels has reached 12°C.

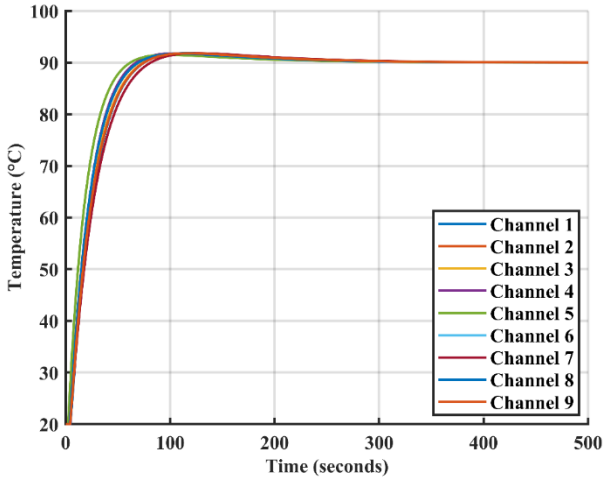

Fig. 9. The multi-channel control effects of PID algorithm under condition 2

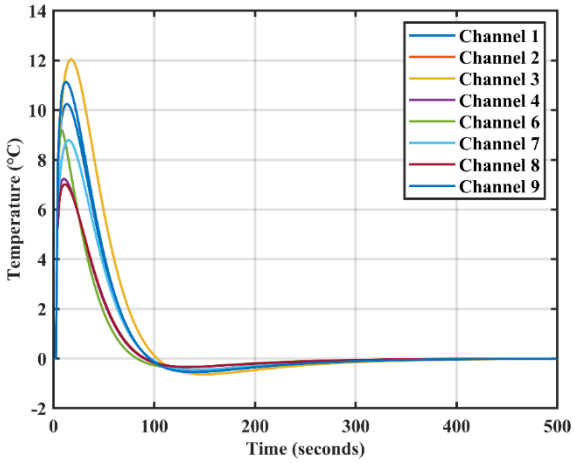

Fig. 10. The temperature difference of PID algorithm under multi-channel condition 2

Based on the PID control in Fig. 9 and Fig. 10, we further integrated the average temperature feedback technique into the PID controller. Fig. 11 shows the control effects of the ATF-PID under Condition 2. It can be observed that although all nine channels exhibit some overshoot, the temperature consistency among the channels has been enhanced. As shown in Fig. 12, the temperature difference between Channel 5 and the other channels has decreased from the previous maximum of 12°C to within 8°C. This demonstrates that the proposed method can effectively ensure temperature consistency among channels during the heating process under different PID control parameters.

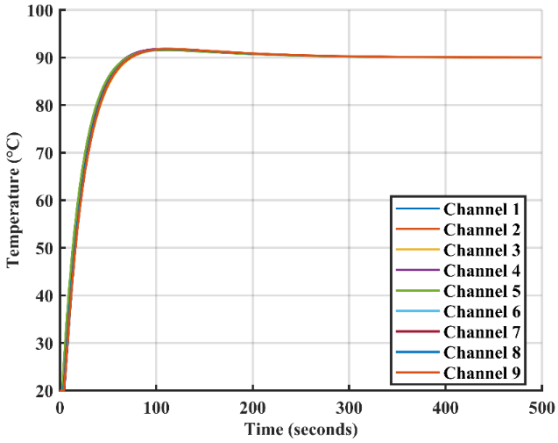

Fig. 11. The multi-channel control effects of ATF-PID algorithm under condition 2

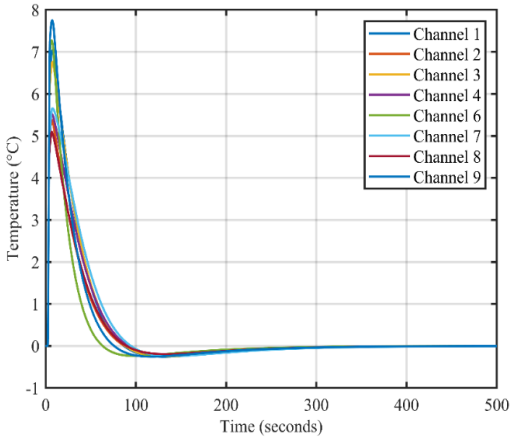

Fig. 12. The temperature difference of ATF-PID algorithm under multi-channel condition 2

5 Experiment Result

In this section, the proposed method is applied to a real multi-channel temperature control system and evaluate its performance by comparing it with the traditional PID method.

5.1 Experiment Setup

In this experiment, a multi-channel temperature control system was set up in thermal vacuum environment, as shown in Fig. 13. Firstly, eight heating plates were mounted on the surface of the DUT in two rows and four columns, with sensors attached to the inner side of the DUT, directly opposite the heating plates. Then, both the sensors and heating plates were connected to the temperature acquisition circuit and power control circuit in the control room, respectively. These circuits were interconnected via EtherCAT network, which allows for synchronized control. The time interval for temperature acquisition and control is one second. In this experiment, the proposed algorithm uses the same coefficient parameters as the traditional PID control algorithm to facilitate comparison of the effects:

$$\begin{cases} K_P = 0.04 \\ K_I = 0.0015 \\ K_D = 0.001 \end{cases}. \tag{25}$$

The DUT, along with the sensors and heating plates attached to it, was placed inside a vacuum chamber. After sealing the chamber, the vacuum operation began. When the pressure inside the vacuum chamber dropped to 10 $\times 10^{-4}$Pa, liquid nitrogen was introduced into the interlayer of the vacuum chamber walls to provide the thermal sink. Meanwhile, the temperature control algorithm was activated and maintained at 22°C. Once the chamber wall temperature stabilizes at -170°C, the heating experiment started.

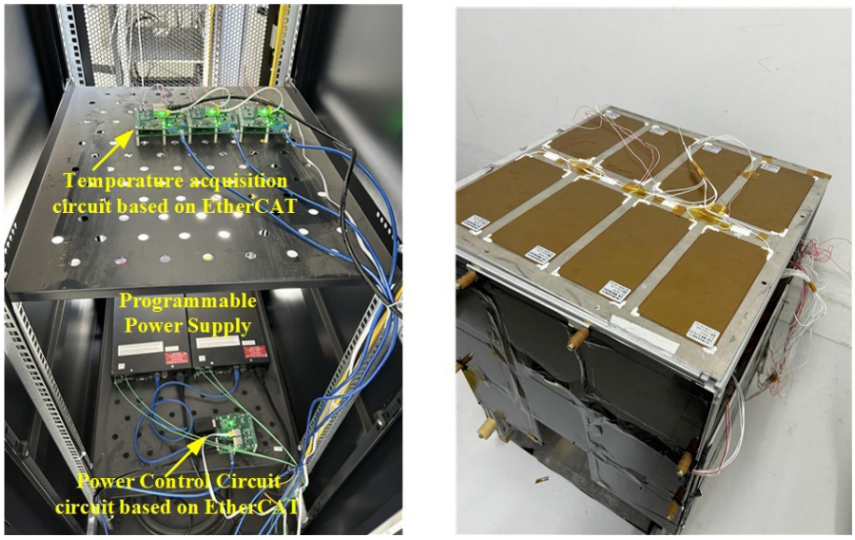

Fig. 13. Experiment setup: control circuit (left), DUT and heating plate (right)

5.2 Experiment Result

Due to the fact that the temperature differences among channels in a multi-channel temperature control process are mainly significant during the heating phase, this experiment primarily observes the phase where the temperature rises from 22°C to 90°C.

Fig. 14 and Fig. 15 show the temperature control effects on the DUT using the traditional PID algorithm and the ATF-PID algorithm, respectively, in the experimental environment mentioned above. It can be seen that the ATF-PID also plays a role in reducing the temperature differences between channels during actual heating control. Fig. 16 and Fig. 17 record the temperature differences between channels during the heating process for these two methods, respectively. It can be seen that, the ATF-PID algorithm reduces the temperature difference from the range of [-4, 6] in the PID algorithm without average temperature feedback to the range of [-2, 3], significantly improving the temperature consistency in the multi-channel heating process.

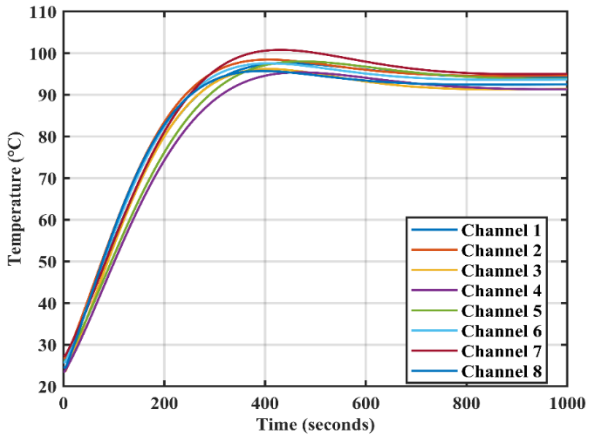

Fig. 14. The multi-channel control effects of PID algorithm in experiment

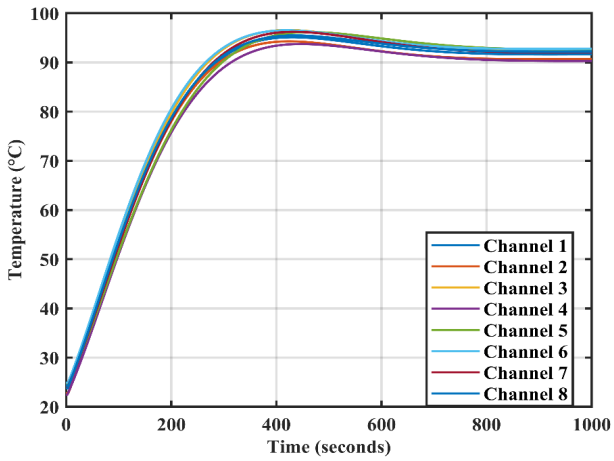

Fig. 15. The multi-channel control effects of ATF-PID algorithm in experiment

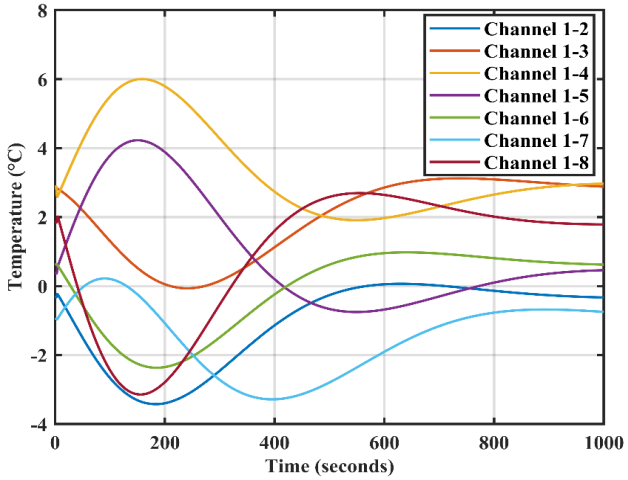

Fig. 16. The temperature difference of PID algorithm for multi-channel heating in experiment

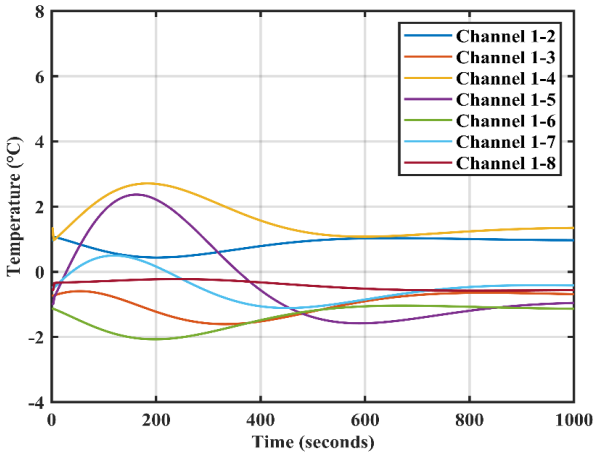

Fig. 17. The temperature difference of ATF-PID algorithm for multi-channel heating in experiment

6 Conclusion

In this article, an average temperature feedback based PID controller is proposed to reduce the temperature difference among the channels for thermal vacuum test. This method calculates the average of the output responses from all channels and feeds back the difference between each channel's output response and the average to the error input of the PID controller, thereby adjusting the heating rate of each channel in real time to achieve overall balanced heating. Compared to the traditional PID algorithm, which lacks average temperature feedback and results in larger temperature differences between different channels, the ATF-PID algorithm not only minimizes these differences but also enhances the overall stability and robustness of the system. Through simulation and real experiments, the proposed ATF-PID algorithm has demonstrated significant improvements in temperature control for multi-channel systems, effectively reducing temperature deviations among channels and ensuring greater consistency during the heating process.

7 Acknowledgement

This work was supported in part by the National Science Foundation of Beijing under Grant 3164043 and in part by the Beijing Science and Technology Projects of Beijing Municipal Education Commission under Grant KM201911232012.

References

[1] R. Dunwoody, J. Reilly, D. Murphy, M. Doyle, J. Thompson, G. Finneran, L. Saloman, C. O'Toole, S.K. Reddy Akarapu, J. Erkal, J. Mangan, F. Marshall, E. Somers, S. Walsh, D. de Faoite, M. Hibbett, D. Palma, L. Franchi, L. Ha, L. Hanlon, D. McKeown, W. O'Connor, A. Uliyanov, R. Wall, B. Shortt, S. McBreen, Thermal vacuum test campaign of the EIRSAT-1 engineering qualification model, Aerospace 9(2)(2022) 99.

[2] K.C. Chin, N.W. Green, E.J. Brandon, Evaluation of supercapacitors for space applications under thermal vacuum conditions, Journal of Power Sources 379 (2018) 155-159.

[3] Y. Wang, Z. Liu, Development of numerical modeling and temperature controller optimization for internal heating vacuum furnace, IEEE Access 9(2021) 126765-126773.

[4] J. Ning, J. Shao, Y. Zhou, Y. Liu, Research on Temperature Control Technology of Thermal Vacuum Test in Aerospace Field, in: Proc. 2018 MATEC Web of Conferences, 2018.

[5] M.A. McCullar, Thermal vacuum testing: test preparation, in: Proc. 2010 Thermal Fluids Anal Workshop (TFAWS 2010), 2010.

[6] J. Zhang, J. Xie, Y. Wang, Y. Pei, The application and the development trend of the measurement and control system in the spacecraft vacuum thermal test, Spacecraft Environment Engineering 29(3)(2012) 263-267.
[7] J.S. Almeida, M.B. Santos, D.L. Panissi, E.C. Garcia, Effectiveness of low-cost thermal vacuum tests of a micro-satellite, Acta Astronautica 59(6)(2006) 483-489.
[8] M. Eilenberger, H. Gunasekar, D.G. Toro, C. Bansch, Analysis of the thermal design of a COTS-based modular battery system for satellites by thermal vacuum testing, CEAS Space Journal 16(4)(2024) 511-523.
[9] Z. Liu, S. Li, G. Liu, Temperature Control of Thermal Vacuum Test Equipment, Electronic Product Reliability and Environmental Testing 30(4)(2012) 1-5.
[10] R.P. Borase, D.K. Maghade, S.Y. Sondkar, S.N. Pawar, A review of PID control, tuning methods and applications, International Journal of Dynamics and Control 9(2021) 818-827.
[11] W.V. Jahnavi, J.N.C. Sekhar, A.S. Reddy, A Review on PID Controller Tuning Using Modern Computational Algorithms, Journal of Emerging Technologies and Innovative Research (JETIR) 10(8)(2023) 160-168
[12] S.A. Ibrahim, E. Yamaguchi, Thermally induced dynamics of deployable solar panels of nanosatellite, Aircraft Engineering and Aerospace Technology 91(7)(2019) 1039-1050.
[13] T.A.M. Euzebio, A.S. Yamashita, T.V.B. Pinto, P.R. Barros, SISO approaches for linear programming based methods for tuning decentralized PID controllers, Journal of Process Control 94(2020) 75-96.
[14] J.-G. Juang, M.-T. Huang, W.-K. Liu, PID control using presearched genetic algorithms for a MIMO system, IEEE Transactions on Systems, Man, and Cybernetics, Part C (Applications and Reviews) 38(5)(2008) 716-727.
[15] B. Yao, C. Jiang, Advanced motion control: From classical PID to nonlinear adaptive robust control, in: Proc. 2010 The 11th IEEE International Workshop on Advanced Motion Control (AMC), 2010.
[16] J.-W. Jung, V.Q. Leu, T.D. Do, E.-K. Kim, H.H. Choi, Adaptive PID speed control design for permanent magnet synchronous motor drives, IEEE Transactions on Power Electronics 30(2)(2014) 900-908.
[17] K.J. Astrom, K.H. Johansson, Q.-G. Wang, Design of decoupled PID controllers for MIMO systems, in: Proc. 2001 The 2001 American Control Conference, 2001.
[18] Y. Wang, Y. Hou, Z. Lai, L. Cao, W. Hong, D. Wu, An adaptive PID controller for path following of autonomous underwater vehicle based on Soft Actor–Critic, Ocean Engineering 307(2024) 118171.
[19] O. Rodríguez-Abreo, J. Rodríguez-Reséndiz, C. Fuentes-Silva, R. Hernández-Alvarado, M.D.C.P.T. Falcón, Self-tuning neural network PID with dynamic response control, IEEE Access 9(2021) 65206-65215.
[20] Z. Haiyang, S. Yu, L. Deyuan, L. Hao, Adaptive neural network PID controller design for temperature control in vacuum thermal tests, in: Proc. 2016 Chinese Control and Decision Conference (CCDC), 2016.
[21] K.K. Tan, S. Huang, R. Ferdous, Robust self-tuning PID controller for nonlinear systems, Journal of process control 12(7)(2002) 753-761.
[22] M. Schwenzer, A. Muzaffer, B. Thomas, A. Dirk, Review on model predictive control: An engineering perspective, in: Proc. the International Journal of Advanced Manufacturing Technology 117(5)(2021) 1327-1349.
[23] F.B. Li, L.H. Yang, A. Ye, Z.M. Zhao, B.X. Shen, Grouping Neural Network-Based Smith PID Temperature Controller for Multi-Channel Interaction System, Electronics 13(4)(2024) 697.
[24] Y. Bai, D. Wang, Fundamentals of fuzzy logic control—fuzzy sets, fuzzy rules and defuzzifications, Advanced fuzzy logic technologies in industrial applications (2006) 17-36.
[25] S.S. Kumar, T. Indiran, G.V. Itty, P.S. J, T.V. Paul, Development of a nonlinear model predictive control-based nonlinear three-mode controller for a nonlinear system, ACS omega 7(46)(2022) 42418-42437.
[26] Y.L. Huang, H.H. Lou, J.P. Gong, T.F. Edgar, Fuzzy model predictive control, IEEE Transactions on Fuzzy Systems 8(6)(2000) 665-678.
[27] K. Jun, W.J. Meng, A. Abraham, H.B. Liu, An adaptive PID neural network for complex nonlinear system control, Neurocomputing 135(2014) 79-85.
[28] L. Zhang, S. Li, Y. Xue, H. Zhou, Z.Y. Ren, Neural network PID control for combustion instability, Combustion theory and modelling 26(2)(2022) 383-398.
[29] K. Cheon, J. Kim, M. Hamadache, D. Lee, On replacing PID controller with deep learning controller for DC motor system, Journal of Automation and Control Engineering 3(6)(2015) 1-5.
[30] H. Kohler, B. Clement, T. Chaffre, G.L. Chenadec, PID tuning using cross-entropy deep learning: A Lyapunov stability analysis, IFAC-PapersOnLine 55(31)(2022) 7-12.
[31] X.S. Wang, Y.H. Cheng, S. Wei, A proposal of adaptive PID controller based on reinforcement learning, Journal of China University of Mining and Technology 17(1)(2007) 40-44.
[32] W.P. An, H.Q. Wang, Q.Y. Sun, J. Xu, Q.H. Dai, L. Zhang, A PID controller approach for stochastic optimization of deep networks, in: Proc. 2018 Proceedings of the IEEE conference on computer vision and pattern recognition, 2018.
[33] Y.P. Zheng, T. Li, Y.F. Sun, D. Su, W.Q. Zhu, S. Xue, J.H. Chen, L.M. Jin, Design of a Multi-Channel PID Temperature Control System Based on PLC and Internet of Things (IOT), Journal of Electrical Engineering & Technology (2024) 1-15.
[34] A. Punse, S. Nangrani, R. Jain, A Novel Application of Multipoint Temperature Control Using PID, in: Proc. 2019 3rd International Conference on Computing Methodologies and Communication (ICCMC), 2019.